Available online at www.sciencedirect.com
ScienceDirect
Remote Sensing of Environment 112 (2008) 1488–1496
Remote Sensing of Environment
www.elsevier.com/locate/rse

Sensitivity of the Indian Ocean circulation to phytoplankton forcing using an ocean model

Bulusu Subrahmanyam [a,*], Kyozo Ueyoshi [b], John M. Morrison [c]

[a] Marine Science Program and Department of Geological Sciences, University of South Carolina, 701 Sumter Street, EWS 617, Columbia, SC 29208 USA
[b] Scripps Institution of Oceanography, University of California, La Jolla, California, USA
[c] Center for Marine Science, University of North Carolina Wilmington, Wilmington, NC, USA

Received 22 August 2006; received in revised form 10 May 2007; accepted 27 May 2007

Abstract

Most ocean general circulation models (OGCMs) do not take into account the effect of space- and time-varying phytoplankton on solar radiation penetration, or do it in a simplistic way using a constant attenuation depth, even though one-dimensional experiments have shown potential significant effect of phytoplankton on mixed-layer dynamics. Since some ocean basins are biologically active, it is necessary for an OGCM to take water turbidity into account, even if it is not coupled with a biological model. Sensitivity experiments carried out with the Massachusetts Institute of Technology (MIT) OGCM with spatially and temporally-varying pigment concentration from Sea-viewing Wide Field-of-view Sensor (SeaWiFS) data during 1998–2003 reveal the effect of ocean turbidity on tropical Indian Ocean circulation. Variations of light-absorbing phytoplankton pigments change the vertical distribution of solar heating in the mixed layer, thereby affecting upper-ocean circulation. A simulation was performed from 1948 to 2003 with a constant minimum pigment concentration of 0.02 mg m^{-3} while another simulation was performed from September 1997 to December 2003 with variable pigment concentration, and the differences between these two simulations allow us to quantify the effects of phytoplankton on solar radiation penetration in the ocean model. Model results from a period of 6 years (1998–2003) show large seasonal variability in the strength of the meridional overturning circulation (MOC), meridional heat transports (MHT), and equatorial under current (EUC). The MOC mass transport changes by 2 to 5 Sv (1 Sv = 10^6 m^3 s^{-1}) between boreal winter (January) and boreal summer (July), with a corresponding change in the MHT of ~0.05 PW (1 PW = 10^{15} W) in boreal winter, which is close to the expected change associated with a significant climate change [Shell, K., Frouin, R., Nakamoto, S., & Somerville, R.C.J. (2003): Atmospheric response to solar radiation absorbed by phytoplankton. *Journal of Geophysical Research, 108*(D15), 4445. doi:10.1029/2003JD003440.]. In addition, changes in phytoplankton pigments concentration are associated with a reduction in the EUC by ~3 cm s^{-1}. We discuss the possible physical mechanisms behind this variability, and the necessity of including phytoplankton forcing in the OGCM.

Keywords: Phytoplankton; Chlorophyll; MIT model; OGCM; Indian Ocean; Meridional overturning circulation (MOC)

1. Introduction

In many Ocean General Circulation Model (OGCM) simulations, biology is generally neglected or crudely taken into account. Solar radiation is either absorbed at the surface assuming the ocean acts as a "blackbody" or decays with a constant attenuation depth. In the real ocean, the presence of phytoplankton modifies attenuation depth, and phytoplankton biomass, hence solar penetration is variable in space and time.

One-dimensional models suggest that phytoplankton, by absorbing solar radiation, may substantially affect upper-ocean dynamics (e.g., Denman, 1973; Schneider & Zhu, 1998). Sathyadranath et al. (1991) used remotely-sensed ocean color data and a Kraus–Turner mixed-layer model to show that the seasonal evolution of sea surface temperature (SST) is influenced by the distribution of phytoplankton. They calculated the net change in heating due to biological processes to be ~4 K per month in the Arabian Sea. In the tropical oceans, Reed (1983) showed that absorption of solar radiation is the dominant source term in the heat budget.

Recently, using satellite ocean-color imagery, absorption of solar radiation by phytoplankton was incorporated in OGCMs to

* Corresponding author. Tel.: +1 803 777 2572; fax: +1 803 777 6610.
E-mail address: sbulusu@geol.sc.edu (B. Subrahmanyam).

0034-4257/$ - see front matter © 2007 Elsevier Inc. All rights reserved.
doi:10.1016/j.rse.2007.05.021

study their effects in the presence of advection (Frouin et al., 2000; Nakamoto et al., 2000, 2001). They found a large-scale amplification of the SST seasonal cycle, typically on the order of 20%, due to phytoplankton. The amplification reached 1.5 K in some regions where the mixed layer was shallow. Murtugudde et al. (2002) argued that the problem of a colder than observed cold tongue in the eastern Equatorial Pacific in model simulations can be remedied by using an accurate solar heating parameterization. Nakamoto et al. (2001) showed that the biologically modulated distributions of solar short-wave heating resulted in shallower mixed-layer depth, enhanced westward near-surface flows, and enhanced flow in the EUC, leading to biomass related cold SST anomalies in the central and eastern Pacific as compared to simulations without phytoplankton in the ocean. Recent model experiments performed by Ueyoshi et al. (2003, 2005) using the MIT OGCM with SeaWiFS chlorophyll concentration data produced the results remarkably similar to those described by Nakamoto et al. (2001). Kara et al. (2004) concluded that single Jerlov water types (Jerlov, 1976) couldn't be used for predicting stratification and surface currents in the Black Sea by demonstrating the impact of using the satellite derived attenuation depth climatology that is easily applied in any OGCM that has fine vertical resolution near the surface. Mobley (1994) showed that chlorophyll concentration ranges from 0.01 mg m^{-3} for clearest open waters to 10 mg m^{-3} for the productive coastal upwelling regions with the near surface globally averaged open ocean value of about 0.5 mg m^{-3}. In all these studies, the heating changes due to phytoplankton resulted in dynamical changes, such as anomalous currents and upwelling. The observed impact of this heating on climate, locally and remotely, is expected to be significant, as suggested by the NCAR Community Climate Model (CCM-3) simulations of Shell et al. (2003).

The motivation of this paper is to use SeaWiFS derived chlorophyll data in the MIT OGCM to show that in ocean basins with significant biological activity, such as the Indian Ocean, the effects of water turbidity in OGCM simulations can have significant effects, even when these simulations are performed using an OGCM without an explicit biological model in the ocean. The principle goal of this study is to assess the role of phytoplankton on the dynamics of the Indian Ocean circulation (meridional overturning circulation (MOC), meridional heat transport (MHT), equatorial Jets and the Equatorial Undercurrent (EUC)). Our hypothesis is that the presence of phytoplankton in the upper ocean, indirectly (and possibly directly) plays a significant role in the variability of circulation of the Indian Ocean. In particular, changes in the physical state of the ocean due to phytoplankton concentrations can be inferred in model simulations using SeaWiFS ocean color data.

2. Model experiments

Simulations were performed using the MIT OGCM (Marshall et al., 1997a,b) with a global $1°\times1°$ horizontal grid extending from 80°S to 80°N, with 23 z-coordinate vertical levels. The upper ~100 m of the model ocean, where solar radiation is absorbed, consists of levels with thicknesses 10 m, 10 m, 15 m, 20 m, 20 m and 25 m. The model incorporates a K-Profile Parameterization (KPP) mixing scheme (Large et al., 1994) and an implementation of a sub-grid isoneutral Redi diffusion scheme (Redi, 1982), and an eddy-induced tracer transport scheme (Gent–McWilliams scheme, Gent & McWilliams, 1990) to conserve water masses (i.e., salinity and temperature) in climate change simulations.

The model is forced with NCEP/NCAR re-analysis (Kalnay et al., 1996; Kistler et al., 2001) of twice-daily wind stress components, daily evaporation minus precipitation, short-wave heat flux and total surface heat flux excluding short-wave heat flux during 1948–2003. The temperature in the top model level is restored towards Reynolds's monthly temperature (Reynolds et al., 2002) for 1948–2003 with a relaxation period of one month, and sea surface salinity is nudged to Levitus monthly climatology (Levitus & Boyer, 1994a,b) with the same relaxation period, while temperature and salinity in the lower levels are dynamically predicted without such a constraint. This model formulation does not have an explicit mixed layer depth (MLD).

In the parameterization proposed by Morel and Antoine (1994), the vertical profile of short-wave radiative heating rate within the upper ocean depends upon chlorophyll pigment concentration, allowing the vertical profile of heating rate to be predicted by introducing remotely-sensed pigment concentrations into the model. For this purpose, monthly mean chlorophyll pigment concentrations derived from SeaWiFS ocean color observations are utilized in the Morel and Antoine parameterization. The vertical profile of chlorophyll pigment concentrations at a given geographical location is assumed uniform for the effective depth of the parameterization. The fraction of total irradiance below 750 nm at the surface was set to 0.60 for overcast skies (Morel & Antoine, 1994). Solar zenith angle was set to zero.

For the first experiment (C002), representing a clear water ocean case for 1948–2003, a minimum constant chlorophyll pigment concentration of $c=0.02$ mg m^{-3} was used in the Morel and Antoine (1994) scheme and the model simulations were initialized with Levitus climatological temperature (T) and salinity (S) from a state of rest at January 1, 1948 and integrated for 56 years.

The e-folding light attenuation depth scale for a water body with chlorophyll concentrations $c=0.02$ mg m^{-3} was estimated from Morel and Antoine (1994) who describe the effective attenuation coefficient, K_{tot}, for net downwelling irradiance when all radiations contained within the whole solar spectrum are considered. The e-folding depth scale for the penetration of the total net downwelling irradiance, defined here as $1/K_{tot}$, is found to be ~25 m when $c=0.02$ mg m^{-3}. A water body with $c=0.02$ mg m^{-3} in Morel and Antoine's scheme approximately corresponds to Jerlov's Type I water which has an attenuation depth of 23 m (Paulson and Simpson, 1977). Fig. 1 shows the normalized vertical profiles of Paulson's in solid lines (Type I–III) and Morel and Antoine's in dashed lines ($c=0.02$–2.0). Two solid lines from right are Types I and IA. Type IA is located to the left of Type I in the upper 50 m showing Type IA is more turbid than Type I. Also Morel's profile with $C=0.02$ mg m^{-3} is plotted which is closer to Type I than to Type IA. Hence, we treated that $c=0.02$ mg m^{-3} represents clear water.

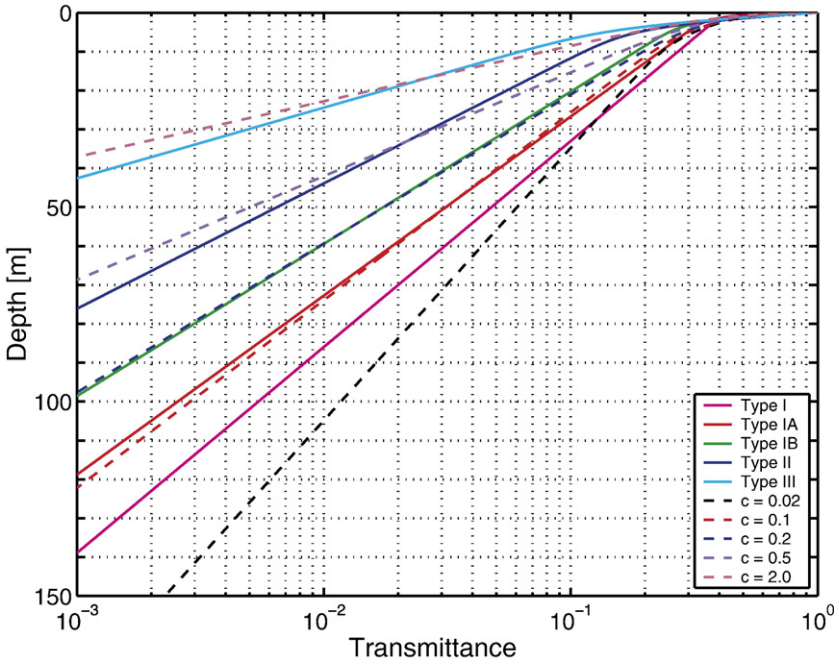

Fig. 1. Vertical profiles of total net downwelling solar irradiance normalized with respect to irradiance just below the surface. Dashed lines represent profiles for various chlorophyll concentrations (mg m^{-3}) proposed by Morel and Antoine (1994). Solid lines represent profiles proposed by Paulson and Simpson (1977) corresponding to various water types defined by Jerlov (1976).

For the second experiment, representing an ocean with realistic chlorophyll concentration (CHL), the model simulation was initialized with the model state (T, S, U, V, etc.) of the clear water experiment (C002) at the end of August, 1997 with the simulation continuing through the end of 2003. Spatially varying monthly mean global SeaWiFS chlorophyll observations were derived from nominal 8-day composite imagery (Yoder & Kennelly, 2003) for each month for the period of September 1997 through the end of 2003. We used these monthly SeaWiFS fields generated from the 8-day composite imagery as external chlorophyll forcing field. CHL experiment starts in September 1997 (the first month SeaWiFS chlorophyll data is available) and ends in December 2003. Monthly chlorophyll data were used with the Morel and Antoine scheme to compute the vertical heating rate of the upper ocean, replacing the minimum uniform constant value used in the clear water body experiment (C002). Fig. 2 shows an example of how the solar irradiance transmittance changes as function of depth along the 10.5°S latitude and 61.5°E longitude sections in the Indian Ocean with the distribution of chlorophyll during August, 2000. The vertical profile of the downwelling irradiance is computed from the chlorophyll-dependent parameterization by Morel and Antoine (1994). We would notice short-wave penetration varies with depth depending on amount of chlorophyll which varies in time and also location. Whereas in C002 experiment, the chlorophyll concentration is independent of time and space, i.e., it is uniform everywhere at all times. The remainder of the model setup was identical for both experiments for the simulation period of September 1997–December 2003. While global simulations were carried out, here a comparison is made between the model simulations (experiments C002 and CHL) for the Indian Ocean (30°E–130°E, 25°N–30°S) for the 6-year period of January 1998 to December 2003.

3. Results

3.1. Meridional overturning circulation (MOC)

The size of the MOC in the Indian Ocean is an important feature of the large-scale ocean circulation. Direct observation of the MOC is extremely difficult, and while a consistent picture of the mean MOC has begun to emerge, little is known about its fluctuations and their effect on the climate. In general, OGCM's do not reproduce strong overturning circulation. Recent improvements in numerical ocean models have stressed the reduction of horizontal and vertical mixing coefficients within the models to match observed values of ocean mixing. The zonally integrated transport is most frequently used to characterize the strength of the thermohaline circulation although it can neither be observed directly nor it easy to interpret (Wunsch, 1997). The mean deep MOC of the Indian Ocean and its associated heat transports are still a matter of much scientific debate with conflicting results depending on the observations and method of analysis used. Two types of MOC have been observed in the Indian Ocean, one has deep water flowing into the basin from south with a compensating outflow at intermediate depths (Schott & McCreary, 2001), the other MOC involves shallower circulations that carry thermocline water from subduction areas in the Southern Hemisphere to the upwelling regions of the equator (Schott & McCreary, 2001). An example of the deep MOC has the Antarctic Bottom Water (ABW) and Circumpolar Deep Water (CDW) entering the

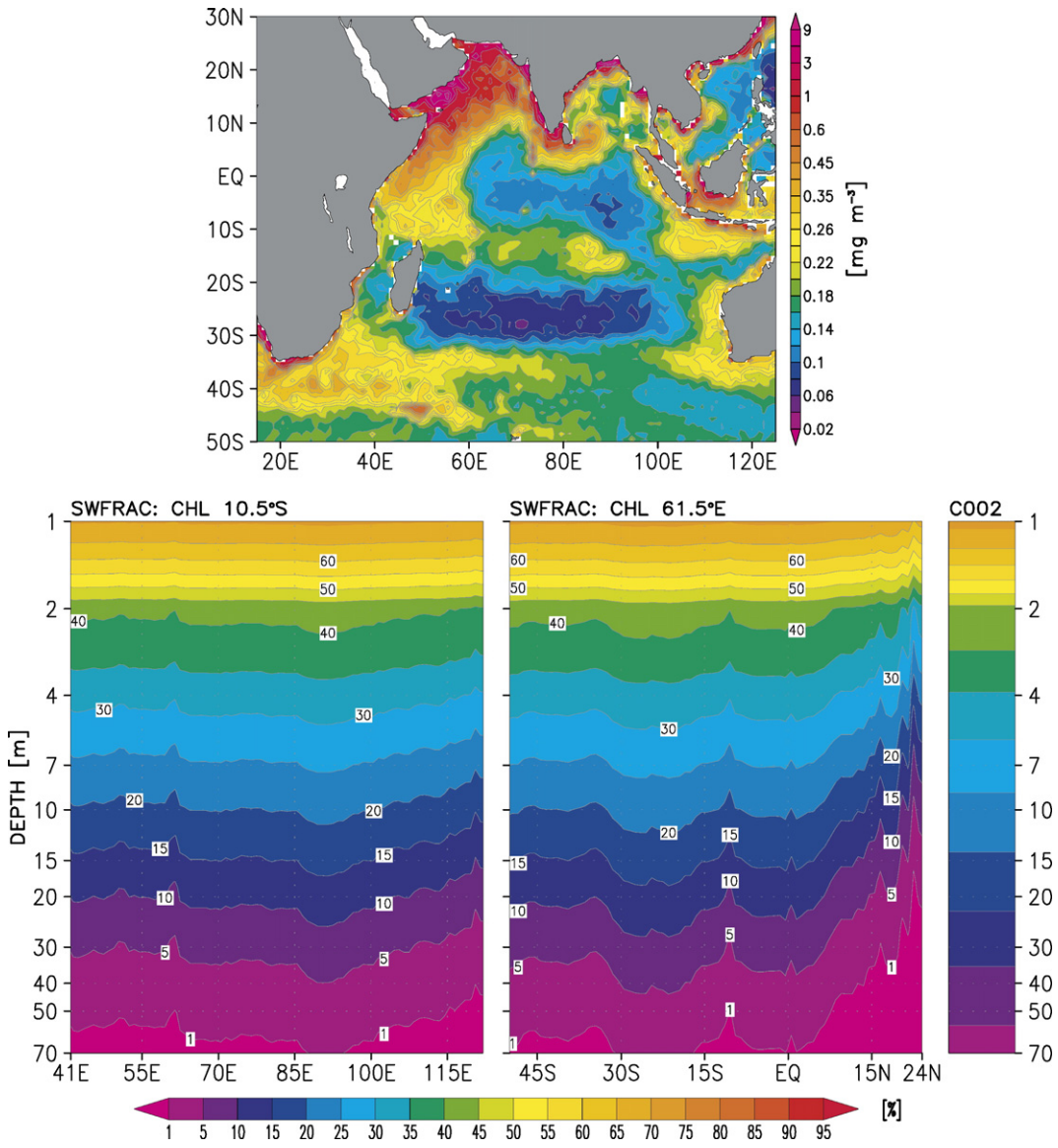

Fig. 2. Short-wave differential heating in the Indian Ocean for the CHL experiment. (Top Panel) SeaWiFS chlorophyll distribution during August, 2000. (Bottom Left) Zonal cross-section at 10.5°S of short-wave radiation that remains unabsorbed at a given depth. It is normalized with the incident short-wave radiation at the ocean surface. (Bottom Right) As in the above panel, except that the meridional cross-section at 61.5°E.

Indian Ocean west of Madagascar and east of Africa and along the ninety East Ridge (Schott & McCreary, 2001).

Stream functions of the zonally integrated transport for the Indian Ocean for the case of CHL simulations are presented in Fig. 3(a,b). There is a shallow "equatorial roll" (particle trajectories show a shallow vertical loop) north of equator at 50 m with a northward transport of ~16 Sv and on the equator close to surface there is an upwelling cell with transports of ~−2 Sv during January (Fig. 3a). In July there is a downwelling cell close to the surface with transports of ~+2 Sv (Fig. 3b). The equatorial rolls, which appear to be in response to the cross-equatorial winds that are present during the monsoon, were first noted by Wacogne and Pacanowski (1996).

The Indian Ocean is strongly dominated by a seasonal overturning cycle. The change of monsoon winds is manifested in a reversal of the MOC throughout the water column (Fig. 3a and b). During the winter monsoon, the deep MOC has strong net northward transport (positive) of ~12–14 Sv in the zonal belt 10°S and 10°N. This northward transport increases with depth. During the summer monsoon (Fig. 3b) the MOC has a net southward transport (negative) of ~22 Sv. There is a strong northward transport at intermediate depths (approximately 1000 m) in January and a recirculation regime with a decrease of northward transport towards north with return flow to the south at shallower depths, but still below the equatorial roll found on the equator.

During the two monsoon seasons, the largest seasonal changes occur near 10°N and 10°S (Fig. 3c, d), which is the region where the seasonal wind stress differences are the largest (Schott & McCreary, 2001). The seasonal wind stress differences result in shallow overturning cells (equatorial rolls) centered on the equator (Wacogne & Pacanowski, 1996) that reverse their sense

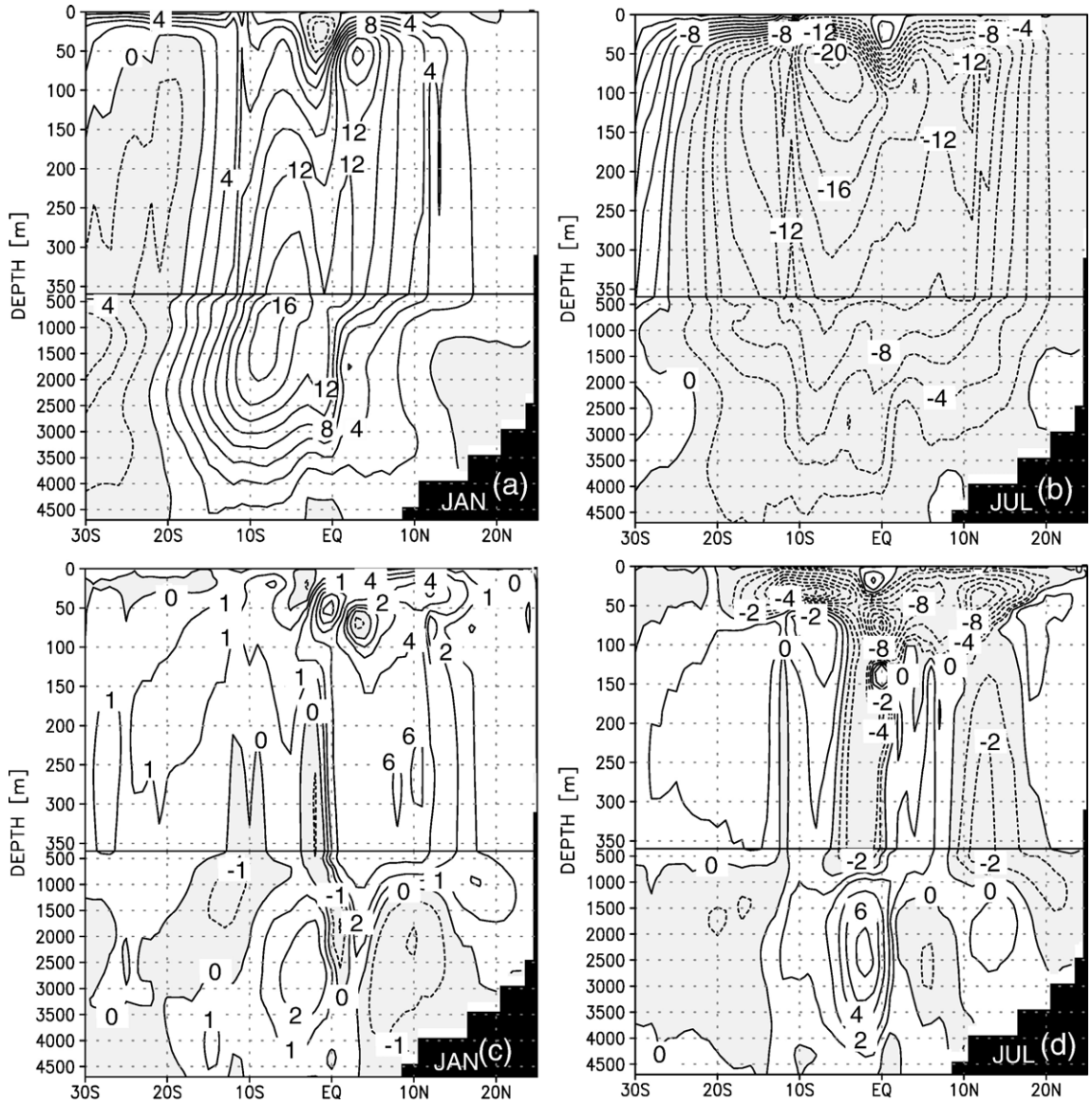

Fig. 3. Seasonal meridional overturning circulation (MOC) for the tropical Indian Ocean along the equator for the CHL simulations during: (a) January and (b) July. Difference in MOC between CHL and C002 simulations during: (c) January and (d) July. Negative values of the stream functions are shaded gray. Units are in Sv (1 Sv=10^6 m^3 s^{-1}) with a contour interval of 2 Sv in (a) and (b), while units are 10^{-1} Sv with a contour interval of 0.2 Sv in (c) and (d).

of rotation from winter to summer in the upper 50 m. The differences in the transport (CHL simulations minus C002 simulations) due to the inclusion of phytoplankton and the associated solar heat penetration into the ocean are large within the upper 100 m within 15° of the equator both in January and July (Fig. 3c, d). Fig. 3c shows that almost +0.8 Sv difference in the equatorial cell during January and a −1.6 Sv difference during July at 100 m (Fig. 3d). Below the equatorial roll both in January and July the changes are on the order of 0.8 Sv.

3.2. Meridional heat transport (MHT)

Previously models of various resolutions and varying physics have been used to study the variability in heat transport for the Indian Ocean (McCreary et al., 1993; Wacogne & Pacanowski, 1996; Garternicht and Schott, 1997; Lee and Marotzke, 1998) with differing results that underscore the large uncertainty in estimates of Indian Ocean meridional transports. Seasonal and annual cycles of the MHT associated with the zonally integrated volume transport are shown from the CHL simulations in Fig. 4a. During January the MHT is about +1.3 PW (northward) at ~7°S, whereas in July (boreal summer) it reaches −2 PW (southward) at ~15°S. The excess annual southward MHT (January minus July) of 0.7 PW between 7°S and 15°S is most likely associated with the transport of warm waters into the Indian Ocean in this zonal belt from the east by the Indonesian Throughflow. The annual cycle shows relatively constant MHT of ~−0.5 PW to the north of ~10°S and ~−1.5 PW at 15°S. Simulations by Wacogne and Pacanowski (1996) show annual mean MHT is −0.55 PW at 13°S, whereas in our simulations we have ~−1.2 PW which is slightly higher than their values because of the 6 years average (1998–2003) we have used in this study. It is interesting to note

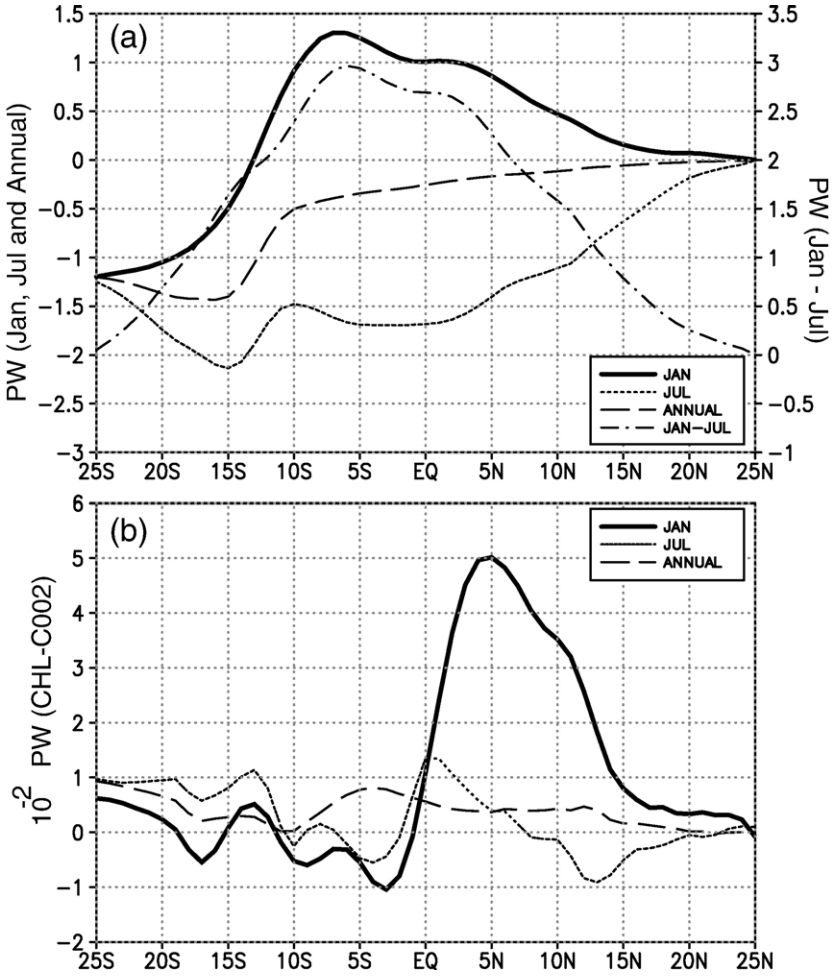

Fig. 4. Meridional heat transport in tropical Indian Ocean. (a) January (dark solid line), July (dashed line), annual (thick dashed line) and January minus July (dashed-dotted line) from the CHL experiment. Left-hand scale in PW (1 PW = 10^{15} W) is for January, July and annual, and right-hand scale in PW for the January minus July. (b) Difference in MHT between two simulations (CHL minus C002) for January, July and annual. Units are 10^{-2} PW.

that the difference between January and July MHT's has a maximum peak-to-peak seasonal cycle of ~3 PW (northward heat transport) at 6°S, which is similar to the model estimates of Jayne and Marotzke (2001). The difference between the CHL and C002 simulations is displayed in Fig. 4b. Large differences are observed in January, reaching a maximum of ~0.05 PW at ~5°N, while the differences in July and over the annual cycle are on the order of 0.01 PW. The observed 0.05 PW increased northward transport is mainly due to change in the advection in the equatorial region caused by the seasonally varying chlorophyll.

3.3. Equatorial jets and undercurrent

Along the equator, the most prominent features are the fall and spring eastward zonal jets, known as the Wyrtki Jets (Wyrtki, 1973) which appear semiannually in the upper-layer along the equator and contribute to the redistribution of mass and heat between the eastern and the western equatorial regions. The Equatorial Indian ocean behaves uniquely compared to the other oceans because of the monsoonal wind features prevailing over this region. The current direction also changes because of the wind reversal. Since the Coriolis force vanishes near the equator the surfacial water is pushed downwind in the wave guide via a Kelvin wave, this jet is referred as Wyrtki Jet. Our model simulations were able to reproduce these features. Fig. 5 shows a longitude-time plot of the equatorial zonal flow along the equator in the surface level (10m deep) for the CHL simulations, as well as the differences between the CHL and C002 simulations. In the CHL simulations (Fig. 5a), the spring jet exists from March to June reaching maximum velocity of 50 cm s^{-1} in May at 76°E. Interestingly, it is evident that the fall jet is strong (60 cm s^{-1}) in November at 65°–70°E and extends eastward up to ~93°E as late as December (Fig. 5a). There is a westward flow both during winter monsoon and summer monsoon periods in this equatorial belt (1°N–1°S). The difference between CHL and C002 simulations (Fig. 5b) displays a velocity difference of ~4 cm s^{-1} during both the spring and the fall jet periods. However, there is a double cell of 4 cm s^{-1} centered at 70°E and 90°E during fall jet period. These jets will have direct impact on the zonal advection of upper-ocean heat content, and any modification of jets' transport will directly affect the heat storage in the eastern Indian Ocean.

In contrast to the equatorial Pacific and Atlantic Oceans where the Equatorial Undercurrent (EUC) persists throughout the year,

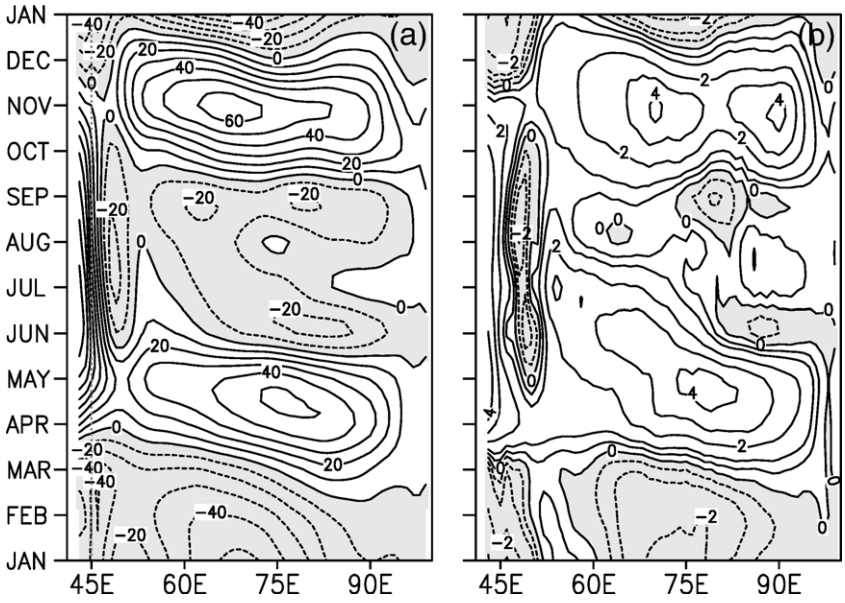

Fig. 5. Time-longitude plot of zonal flow in the surface level (10-m deep) along the equator during January 1998–January 1999, for (a) CHL and (b) difference between two simulations (CHL minus C002). Units are cm s^{-1} with a contour interval of 10 cm s^{-1} in (a), while units are cm s^{-1} with a contour interval of 1 cm s^{-1} in (b).

in the Indian Ocean the EUC is generally observed only during February–April when easterly winds prevail over most of the equatorial basin. In the Indian Ocean, the EUC may not appear in any longitude sections in some years or may appear only in some sections (Knauss & Taft, 1964). In our model simulations the EUC is a robust feature during 1998. In the monthly mean zonal current distribution within the upper 150 m at 72°E on the equator, the EUC appears during March in the CHL simulations with speeds of ~30 cm s^{-1} at ~100 m depth (Fig. 6a).

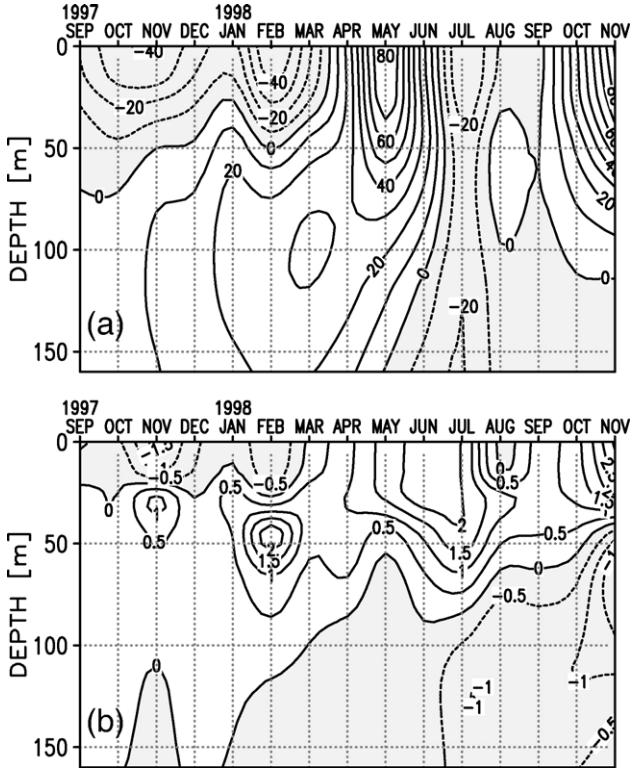

Fig. 6. Monthly mean zonal velocity in upper 150 m at 72°E on the equator for the CHL simulations (a) showing eastward Wyrtki Jets in boreal fall of 1997 and spring of 1998, and eastward EUC during February–May 1998 and at weaker EUC at shallow depth in August 1998. The difference between two simulations (CHL minus C002) is shown in (b). Units are cm s^{-1} with a contour interval of 10 cm s^{-1} in (a), while units are cm s^{-1} with a contour interval of 0.5 cm s^{-1} in (b).

The model simulated the surface current above the EUC is westward. The strength of EUC depends on how well the model resolves the vertical structure of the thermocline (Maghanani et al., 2003). Observations from the region south of Sri Lanka by Reppin et al. (1999) for the period from June 1993 to August 1994 showed that there was an EUC between 50–150 m from February to May with a velocity at ~50 cm s^{-1} which agrees with our CHL model simulations, though we are showing for year 1998. The model also displays that the EUC in March rises to the surface and merges with the spring Wyrtki Jet by May, and this is in supportive of Bubanov (1994) observations. The model also simulates an eastward flow coinciding with the eastward spring and fall Wyrtki jets in 1998. The absence of fall jet in 1997 appears to be associated with differences in wind field associated with the 1997/98 Indian Ocean Dipole (IOD)(Murtugudde et al., 2000; Saji et al., 1999; Webster et al., 1999). The El Niño event and the associated winds over the equatorial Indian Ocean appear to have subsided by fall 1998. The differences between the two model simulations show higher velocity differences of ~2–3 cm s^{-1} both during the periods of EUC and equatorial jets (Fig. 6b).

4. Conclusions

In this work, a coarse resolution (1° × 1°) primitive OGCM was used to study the effects of space- and time-varying phytoplankton concentration on the upper-ocean dynamics of tropical Indian Ocean. A first multi-year simulation was performed for the period from January 1948 to December 2003 with a constant minimum pigment concentration of 0.02 mg m^{-3} (C002) which is representative of a clear water type, and a second simulation from

September 1997 to December 2003 with a variable pigment concentration (CHL), which mimics a more realistic water type, using the available SeaWiFS ocean color data. The differences between these two experiments (CHL–C002) show the effect of phytoplankton on solar radiation penetration in the ocean model. Comparison of results of these simulations for the 6-year period (1998–2003) shows large seasonal variability in the strength of MOC and the associated heat transport, and in the strength of Equatorial Jets and EUC. The differences (CHL–C002) show changes in the MOC by 0.8 Sv and MHT by 0.05 PW in January, as well as changes in the strength of the Equatorial Jets and EUC (by $\sim$3 cm s^{-1}). The scales of simulated changes in MOC and MHT associated with the effects of phytoplankton are on scales that are of same order as inferred climate variability suggested by *in situ* observations. These findings support previous results obtained with the Ocean isoPYCnal (OPYC) model and pigment concentration from the Coastal Zone Color Scanner (CZCS) (Nakamoto et al., 2001).

Acknowledgements

The authors would like to thank the SeaWiFS project (code 970.2) and the GES DISC DAAC (code 902), Greenbelt, MD 20771, for the production and distribution, respectively, of these data. Use of this data is in accordance with the SeaWiFS Research Data use Terms and Conditions Agreement. The Global SeaWiFS chlorophyll 1997–2003 data used in this study were provided by U. S. JGOFS Data Management Office from their web site at http://usjgofs.whoi.edu/las/servlets/dataset/. This work was supported in part by the NASA Physical Oceanography Program under Grant NNG06GE93G and in part by the South Carolina Space Grant Consortium under Grant 520544-Bulusu.

References

Bubanov, V. A. (1994). Climate zonal pressure gradient in the equatorial zone of the Indian Ocean. *Oceanology*, *33*, 414.

Denman, K. L. (1973). A time-dependent model of the upper ocean. *Journal of Physical Oceanography*, *3*, 173−184.

Frouin, R., Nakamoto, S., Paci, A., Miller, A., & Iacobellis, S. F. (2000). Biological Modulation of Sea Surface Temperature. *Proceedings of Fifth Pacific Ocean Remote Sensing Conference PORSEC, 5–8 December 2000, Goa, India*, *Vol. 2* (pp. 498−501).

Garternicht, U., & Schott, F. (1997). Heatfluxes of the Indian Ocean from a global eddy-resolving model. *Journal of Geophysical Research*, *102*, 21147−21159.

Gent, P. R., & McWilliams, J. C. (1990). Isopycnal mixing in ocean circulation models. *Journal of Physical Oceanography*, *20*, 150−155.

Jayne, S. R., & Marotzke, J. (2001). The dynamics of ocean heat transport variability. *Reviews of Geophysics*, *39*, 385−411.

Jerlov, N. G. (1976). *Marine Optics.* New York: Elsevier Oceanography Series, Elsevier Sci. Publ. Co. 231 pp.

Kalnay, E., Kanamitsu, M., Kistler, R., Collins, W., Deaven, D., Gandin, L., et al. (1996). The NMC/NCAR 40-Year Reanalysis Project. *Bulletin of American Meteorological Society*, *77*, 437−471.

Kara, A. B., Hurlburt, H. E., Rochford, P. A., & O'Brien, J. J. (2004). The impact of water turbidity on the interannual sea surface temperature simulations in a layered global ocean model. *Journal of Physical Oceanography*, *34*, 345−359.

Kistler, R., Kalnay, E., Collins, W., Saha, S., White, G., Woollen, J., et al. (2001). The NCEP-NCAR 50-year reanalysis: Monthly means CD-ROM and documentation. *Bulletin of American Meteorological Society*, *82*, 247−268.

Knauss, J. A., & Taft, B. A. (1964). Equatorial undercurrent of the Indian Ocean. *Science*, *143*, 354−356.

Large, W. G., McWilliams, J. C., & Doney, S. C. (1994). Oceanic vertical mixing: A review and a model with a nonlocal boundary layer parameterization. *Reviews of Geophysics*, *32*, 363−403.

Lee, T., & Marotzke, J. (1998). Seasonal cycle of meridional overturning and heat transport of the Indian Ocean. *Journal of Physical Oceanography*, *28*, 923−943.

Levitus, S., & Boyer, T. P. (1994a). World Ocean Atlas 1994, Vol. 4: Temperature. NOAA Atlas NESDIS 4. Washington, D.C.: U.S. Department of Commerce, 117 pp.

Levitus, S., & Boyer, T. P. (1994b). World Ocean Atlas 1994, Vol. 3: Salinity. NOAA Atlas NESDIS 3. Washington, D.C.: U.S. Department of Commerce, 99 pp.

Maghanani, V., Subrahmanyam, B., Xie, L., & Morrison, J. (2003). Numerical simulation of seasonal and interannual Indian Ocean upper layer circulation using MICOM. *Journal of Geophysical Research*, *108*, 33-1−33-21. doi:10.1029/2002JC001567

Marshall, J., Adcroft, A., Hill, C., Perelman, L., & Heisey, C. (1997a). A finite-volume incompressible Navier–Stokes model for studies of the ocean on parallel computers. *Journal of Geophysical Research*, *102*, 5753−5766.

Marshall, J., Hill, C., Perelman, L., & Adcroft, A. (1997b). Hydrostatic, quasi-hydrostatic and non-hydrostatic ocean modeling. *Journal of Geophysical Research*, *102*, 5733−5752.

McCreary, J. P., Jr., Kundu, P. K., & Molinari, R. L. (1993). A numerical investigation of dynamics, thermodynamics and mixed layer processes in the Indian Ocean. *Progress in Oceanography*, *31*, 181−244.

Mobley, C. D. (1994). *Light and Water: Radiative Transfer in Natural Waters.* New York: Academic Press, 592 pp.

Morel, A., & Antoine, D. (1994). Heating rate within the upper ocean in relation to its bio-optical state. *Journal of Physical Oceanography*, *24*, 1652−1665.

Murtugudde, R., Beauchamp, J., McClain, C. R., Lewis, M. R., & Busalacchi, A. J. (2002). Effects of penetrative radiation on the upper tropical ocean circulation. *Journal of Climate*, *15*, 470−486.

Murtugudde, R., McCreary, J. P., Jr., & Basalacchi, A. J. (2000). Oceanic processes associated with anomalous events in the Indian Ocean with relevance to 1997–1998. *Journal of Geophysical Research*, *105*, 3295−3306.

Nakamoto, S., Prasanna Kumar, S., Oberhuber, J. -M., Ishizaka, J., Muneyama, K., & Frouin, R. (2001). Response of the equatorial Pacific to chlorophyll pigments in a mixed layer-isopycnal ocean general circulation model. *Geophysical Research Letters*, *28*, 2021−2024.

Nakamoto, S., Prasanna-Kumar, S., Oberhuber, J. -M., Muneyama, K., & Frouin, R. (2000). Chlorophyll modulation of sea surface temperature in the Arabian Sea in a mixed layer isopycnal general circulation model. *Geophysical Research Letters*, *27*, 747−750.

Paulson, C. A., & Simpson, J. J. (1977). Irradiance measurements in the upper ocean. *Journal of Physical Oceanography*, *7*, 953−956.

Redi, M. H. (1982). Oceanic isopycnal mixing by coordinate rotation. *Journal of Physical Oceanography*, *12*, 1154−1158.

Reed, R. K. (1983). Heat fluxes over the eastern tropical Pacific and aspects of the 1972 El Niño. *Journal of Geophysical Research*, *88*, 9627−9638.

Reppin, J., Schott, F. A., Fischer, J., & Quadfasel, D. (1999). Equatorial currents and transports in the upper central Indian Ocean: Annual cycle and interannual variability. *Journal of Geophysical Research*, *104*, 15495−15514.

Reynolds, R. W., Rayner, N. A., Smith, T. M., Stokes, D. C., & Wang, W. (2002). An improved in situ and satellite SST analysis for climate. *Journal of Climate*, *15*, 1609−1625.

Saji, N. H., Goswami, B. N., Vinayachandran, P. N., & Yamagata, T. (1999). A dipole mode in the tropical Indian Ocean. *Nature*, *401*, 360−363.

Sathyadranath, S., Gouveia, A. D., Shetye, S. R., Ravindran, P., & Platt, T. (1991). Biological control of surface temperature in the Arabian Sea. *Nature*, *349*, 54−56.

Schneider, E. K., & Zhu, Z. X. (1998). Sensitivity of the simulated annual cycle of sea surface temperature in the equatorial Pacific to sunlight penetration. *Journal of Climate*, *8*, 1932−1950.

Schott, F. A., & McCreary, J. P., Jr. (2001). The monsoon circulation of the Indian Ocean. *Progress in Oceanography*, *51*, 1−123.

Shell, K., Frouin, R., Nakamoto, S., & Somerville, R. C. J. (2003). Atmospheric response to solar radiation absorbed by phytoplankton. *Journal of Geophysical Research*, *108*(D15), 4445. doi:10.1029/2003JD003440

Ueyoshi, K., Frouin, R., Nakamoto, S., & Subrahmanyam, B. (2005). Sensitivity of equatorial Pacific Ocean circulation to solar radiation absorbed by phytoplankton. In R. J. Frouin, M. Babin, & S. Sathyendranath (Eds.), *Remote Sensing of the Coastal Environment. Proc. SPIE*, *Vol. 5885*. doi:10.1117/12.621424

Ueyoshi, K., Stammer, D., Nakamoto, S., Subrahamanuam, B., Prasanna Kumar, S., & Muneyama, K. (2003). Sensitivity of the equatorial Pacific Ocean circulation to chlorophyll modulation of penetrative solar irradiance in a GCM. *IUGG 2003 Scientific Program and Abstracts, Sapporo, Japan, June 30–July 11, 2003, JSP09/11P/B20-002, B.103*.

Wacogne, S., & Pacanowski, R. C. (1996). Seasonal heat transport in a primitive equation model of the tropical Indian Ocean. *Journal of Physical Oceanography*, *26*, 2666−2699.

Webster, P. J., Moore, A. M., Loschnigg, J. P., & Leben, R. R. (1999). Coupled ocean-temperature dynamics in the Indian Ocean during 1997–98. *Nature*, *401*, 356−360.

Wunsch, C. (1997). Response of an equatorial ocean to a periodic monsoon. *Journal of Physical Oceanography*, *7*, 497−511.

Wyrtki, K. (1973). An equatorial jet in the Indian Ocean. *Science*, *181*, 262−264.

Yoder, J. A., & Kennelly, M. A. (2003). Seasonal and ENSO variability in global ocean phytoplankton chlorophyll derived from 4 years of SeaWiFS measurements. *Global Biogeochemical Cycles*, *17*(1112), 23-1−23-14. doi:10.1029/2002GB001942